

## Original Article

# The chicken embryo umbilical artery is a promising *in vivo* model system for the study of vasospasm

Yongjie Yuan, Si Yang, Chao Li, Kan Xu, Qi Luo, Jinlu Yu

Department of Neurosurgery, First Hospital of Jilin University, Changchun 130021, China

Received October 13, 2015; Accepted January 27, 2016; Epub February 15, 2016; Published February 29, 2016

**Abstract:** Objectives: The chicken umbilical artery floats in a fluid environment in the allantoic cavity that is similar to the human cerebral vessels in the subarachnoid space. Therefore, to simulate the pathological changes of cerebral vasospasm (CVS) after subarachnoid hemorrhage (SAH) in humans, this study established an umbilical arterial vasospasm model induced by internal bleeding in the allantoic cavity of chicken embryos. Methods: We established an umbilical arterial vasospasm model using a needle puncture method on a vein in the chorioallantoic membrane (CAM) to induce a hemorrhage in the allantoic cavity of 11-day-old chicken embryonated eggs. The treated chicken embryos were sacrificed on days 1, 3, 5, and 7 post-hemorrhage to collect the umbilical artery samples. The pathological sections were prepared for hematoxylin-eosin (HE) staining, terminal deoxynucleotidyl transferase (TDT)-mediated dUTP nick end labeling (TUNEL) staining, and transmission electron microscope (TEM) observation to investigate the changes in the inner cross-sectional area (CSA), wall thickness, number of TUNEL-positive apoptotic cells in the vascular wall, and wall ultrastructure of the umbilical artery. Results: Compared with the control group, the experimental group showed no statistically significant difference in the inner CSA and wall thickness of the umbilical artery on day 1 post-hemorrhage. On days 3, 5, and 7 post-hemorrhage, the inner CSA of the umbilical artery was significantly smaller ( $P < 0.05$ ), and the umbilical artery had a thicker wall in the experimental group ( $P < 0.05$ ) versus the control group. TUNEL staining of the umbilical arterial sections revealed that, on days 3 and 5 post-hemorrhage, the apoptotic index of the umbilical arterial wall cells in the experimental group was remarkably higher than that in the control group ( $P < 0.05$ ). TEM observation of the umbilical arterial wall on day 5 post-hemorrhage revealed that, in the experimental group, the endothelial cells showed shrinkage and were loosely arranged, the normal intercellular connections were absent, the fragmented nuclear chromatin aggregated toward the nuclear membrane, and the subendothelial elastic layer exhibited wrinkles arranged in a wavy pattern. In the control group, the endothelial cells had oval nuclei and were arranged in a single layer with tight intercellular connections, and the subendothelial layer was evenly arranged and clearly structured. Conclusions: Our chicken embryo umbilical arterial vasospasm model, established by the needle puncture of CAM vessels to induce internal bleeding in the allantoic cavity, exhibits certain pathological changes similar to mammalian SAH-induced CVS, which makes it to be a promising *in vivo* model system for study of vasospasm.

**Keywords:** Cerebral vasospasm, model, subarachnoid hemorrhage, umbilical artery in the allantoic cavity

## Introduction

Aneurysmal subarachnoid hemorrhage (aSAH) accounts for approximately 5-10% of cerebral stroke cases [1, 2]. Cerebral vasospasm (CVS) and the brain damage associated with CVS are believed to be major contributors to the high mortality and disability rates associated with cerebral stroke [3, 4]. CVS typically occurs three days after subarachnoid hemorrhage (SAH), reaches a peak 6-8 days post-SAH, and is maintained at peak levels for 2-3 weeks [5]. Studies of the pathogenesis of CVS generally

involve animal models and propose various hypotheses; however, due to significant variability in the animal models, an animal model that completely simulates the characteristics of post-aSAH human CVS has not been established [6, 7]. Therefore, there is an urgent need for the development and improvement of reliable animal models to explore the pathogenesis of CVS and assess the efficacy of CVS prevention and treatment approaches.

Currently, the most commonly used mammalian CVS models include rat, mouse, rabbit,

## The chick embryo umbilical artery vasospasm model

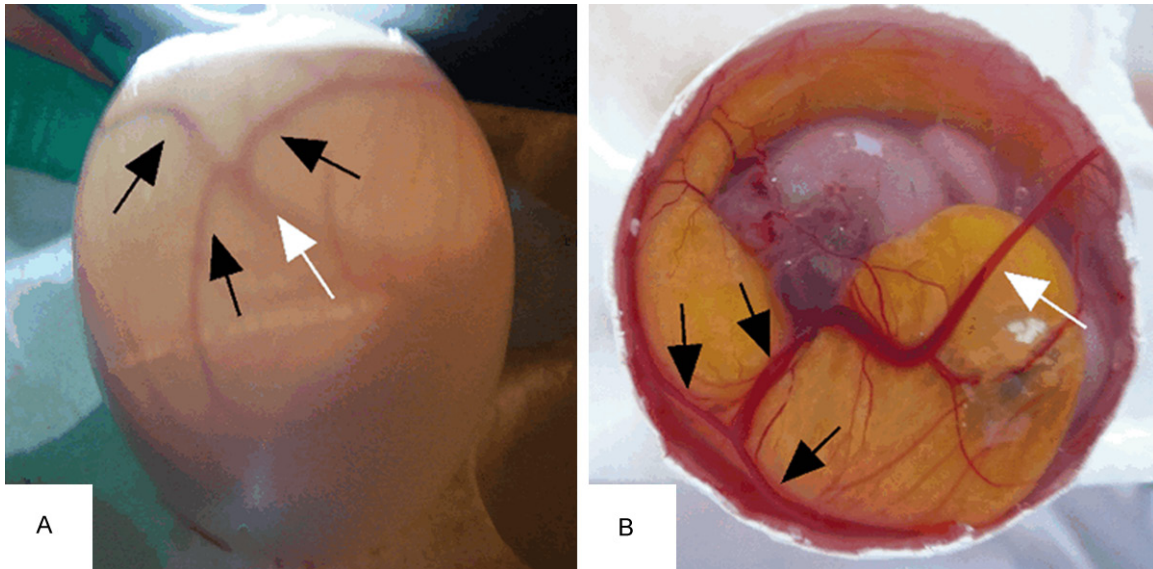


**Figure 1.** A. Candling of the 11-day-old chicken embryonated egg from its blunt end (the air chamber end) indicates that the CAM vessels are clearly visible. At the top of the embryo, a large vein departed the CAM after several CAM vessels (denoted by the black arrows) confluence and extended toward the deep allantoic cavity to connect to the chicken embryo, which is the umbilical vein (denoted by the white arrow); B. The internal anatomical structure of an 11-day-old chicken embryonated egg featuring the umbilical artery and its branches (black arrows) and the umbilical vein (white arrow).

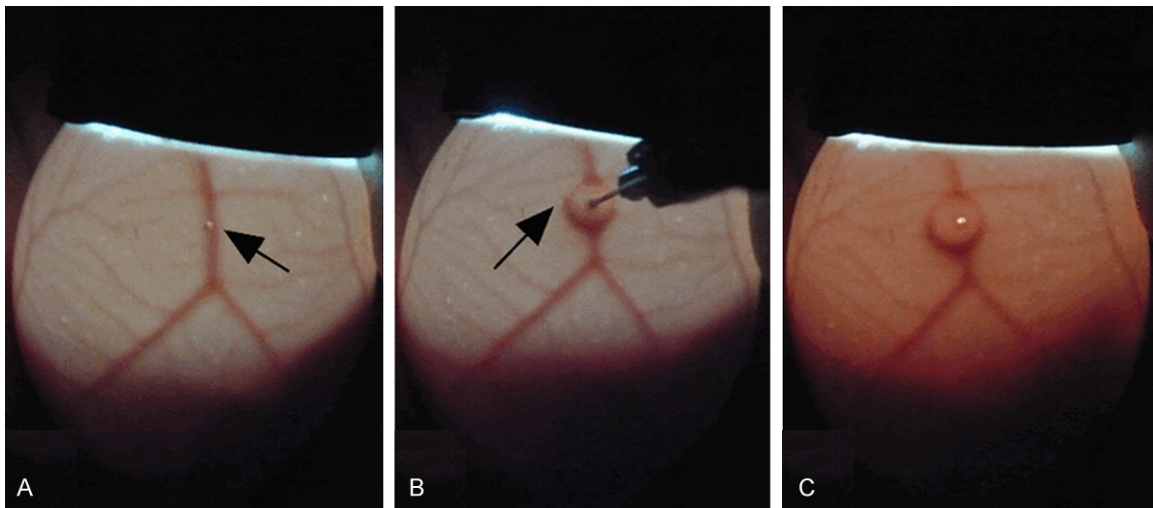


**Figure 2.** A CAM vessels puncture method to cause internal bleeding in the allantoic cavity. A. A 16G syringe needle was used to gently drill through the eggshell without damaging the CAM and vessels (black arrow); B. A 26G syringe needle was used to puncture the CAM vein to cause internal bleeding in the allantoic cavity (black arrow) that could be observed under an egg-candling lamp; C. After needle withdrawal, the chicken embryonated egg was gently rotated to disperse the blood evenly throughout the allantoic cavity until the allantoic fluid became turbid.

canine, and primate (e.g., monkey) models [8]. However, these mammalian models have various shortcomings such as high costs, complicated operations, long rearing periods, and ethical constraints. Among other vertebrates, chickens are the closest to mammals phylogenetically. Chicken embryos have been widely

used in biomedical research. For example, the chorioallantoic membrane (CAM), a thin, highly vascularized transparent membrane structure attached to the inner eggshell surface, has been used extensively in diverse biomedical fields such as pharmacy, regenerative medicine, and oncology [9-12]. However, studies on

## The chick embryo umbilical artery vasospasm model

the umbilical artery and vein, which are connected to the CAM and float in the allantoic cavity, are scarce. The chicken embryo allantoic artery in the allantoic cavity has a fluid environment that is similar to that of human cerebral vessels in the subarachnoid space. Chicken CAM vessels attached to the inner eggshell surface are clearly visible under light and can be easily needle punctured to induce internal bleeding in the allantoic cavity. This method is easy to conduct and observe. Based on this unique feature of the umbilical artery in the allantoic cavity of chicken embryos, we attempted to induce umbilical arterial vasospasm to simulate post-aSAH CVS pathological changes by needle puncturing chicken embryo CAM vessels to cause a hemorrhage in the allantoic cavity.

### Materials and methods

#### *Hatching and sorting the chicken embryonated eggs*

All the animal experimental operations were approved by the Ethics Committee of Jilin University. In this study, 65 specific-pathogen-free (SPF)-grade fresh chicken fertilized eggs (with an average weight of  $60\pm 2.9$  g) were purchased from Beijing Merial Vital Laboratory Animal Technology Co., Ltd. The 24 samples of the control group were randomly divided into 4 subgroups (day 1, 3, 5, 7) with 6 samples in each group; while 36 samples in the experimental group were also divided into 4 subgroups (day 1, 3, 5, 7) with 9 samples in each group; 5 eggs were used as a reserve supply, for gross observation of the chicken embryos, or for verification that CAM needle puncture causes internal bleeding in the allantoic cavity. A fully automated incubator was used to hatch the fertilized eggs. The parameters of the incubator: From 1st to 6th day, the temperature is  $38^{\circ}\text{C}$  and humidity is 60%; From 7th to 12th day, the temperature is  $37.8^{\circ}\text{C}$  and humidity is 55%; From 13th to 18th day, the temperature is  $37.6^{\circ}\text{C}$  and humidity is 60%; rotate the eggs once every 90 min. On the 5th day, an egg-candling lamp was used to observe the chicken embryos in a dark room. The eggs that failed to hatch were discarded and replaced with fertilized eggs from the reserve supply.

#### *Establishment of hemorrhage in the allantoic cavity of the chicken embryo*

On the 11th day of hatching, each chicken embryo was candled from the blunt end (i.e.,

the air chamber) of the egg, and the CAM vessels were found to be clearly visible under an egg-candling lamp. At the top of the chicken embryo, a large vein departed the CAM after multiple vascular branches confluence and extended toward the deep allantoic cavity to connect to the chicken embryo, which is the umbilical vein (**Figure 1A**). A relatively large CAM vessel was selected for needle puncturing. After wiping the surface of the embryonated egg with an alcohol-soaked cotton ball, a 16G syringe needle was used to gently drill through the eggshell without damaging the CAM and vessels, followed by puncture of the selected CAM vessel with a 26G syringe needle. After the hemorrhage became clearly visible under the egg-candling lamp, the egg was gently rotated to disperse the blood evenly throughout the allantoic cavity until the allantoic fluid became turbid (**Figure 2**). In the control group, after drilling through the eggshell with a 16G syringe needle, the fertilized egg was placed back into the incubator for hatching without puncturing a CAM vein. The eggs were candled and observed in succession using the egg-candling lamp daily, and dead chicken embryos were removed.

#### *Gross observation of hemorrhage in the allantoic cavity of the chicken embryo*

It was necessary to preclude any internal bleeding in the allantoic cavity that was caused by destroying the CAM vessel during opening chick eggshell. First, on day 1 post-hemorrhage, the embryonated eggs in both the experimental and control groups were sacrificed by freezing them at  $-80^{\circ}\text{C}$  for 30 min. Next, the air chamber end of the egg was gently opened with tweezers to expose the inner shell membrane and firmly attached CAM. Subsequently, the exposed eggshell membrane and the attached CAM, along with a portion of the eggshell at the air chamber end of the egg, were resected with tissue scissors to determine if the CAM vessel puncture had caused internal bleeding in the allantoic cavity.

#### *Sample collection and fixation of the umbilical artery in the allantoic cavity*

On days 1, 3, 5, or 7 post-hemorrhage, each chicken embryonated egg was carefully opened from the air chamber end with tweezers to expose the inner shell membrane and firmly attached CAM. After gently wiping the inner

## The chick embryo umbilical artery vasospasm model

**Table 1.** Number of post-hemorrhage chicken embryo deaths in the two groups

	Day 1	Day 3	Day 5	Day 7
Control group	0	0	0	0
Experimental group	2 (22.22%)	3 (33.33%)	4 (44.44%)	4 (44.44%)

eggshell membrane with a phosphate-buffered saline (PBS)-wetted cotton swab, the CAM vessels became clearly visible. Be careful to avoid the large vessels, and then gently tear up the inner eggshell membrane and the attached CAM with a 16G syringe needle, pour as much of the allantoic fluid as possible. Subsequently, approximately 10 ml of pre-chilled (4°C) 4% paraformaldehyde (4% paraformaldehyde in 0.1 mol/L PBS (pH 7.4) or 2.5% glutaraldehyde (for observation under a transmission electron microscope (TEM)) was injected into the allantoic cavity, followed by fixation at 4°C for 2 h. After opening the eggshell, the umbilical artery and vein in the allantoic cavity were found to be connected to the ventral side of the chicken embryo. The umbilical artery in the allantoic cavity had bifurcated from its origin (**Figure 1B**). A proximal segment (approximately 1 cm in length) of the right branch following the umbilical arterial bifurcation was collected and placed in 4% paraformaldehyde or 2.5% glutaraldehyde (for TEM observation) for fixation and storage.

### *Measurement of the inner cross-sectional area (CSA) and wall thickness of the umbilical artery*

The umbilical arterial segment fixed in 4% paraformaldehyde was evenly divided into three segments (the proximal, distal, and middle segments) that were separately dehydrated, cleared, embedded, and sectioned to obtain 5- $\mu$ m-thick transverse vascular sections. After hematoxylin-eosin (HE) staining and section sealing, the sections were observed and photographed under a microscope (Olympus), and the resulting images were recorded. Two researchers independently measured the inner and outer CSAs using ImageJ software and averaged the CSAs of the three sections to obtain the CSA value for each artery. The final CSAs were obtained by averaging the results from the two researchers. The wall thicknesses were calculated based on the inner and the outer CSAs using a geometric formula.

### *Terminal deoxyribonucleotidyl transferase (TDT)-mediated dUTP nick end labeling (TUNEL) staining*

TUNEL staining of the paraffin-embedded sections was conducted using TUNEL kits (In Situ Cell Death Detection Kit, POD, Roche, Inc.), rigorously following the manufacturer's instructions. Briefly, the paraffin-embedded sections were dewaxed, rehydrated, washed with PBS solution, and permeabilized with 0.1% Triton-100. Subsequently, the fluorescence-labeled nucleotides were mixed onto the 3'-OH terminal of the fragmented DNA of the apoptotic cells by dropwise adding the TDT and fluorescence-labeled nucleotides onto the sections and incubating them at 37°C for 1 h. After the PBS washes, anti-fluorescein antibody-labeled peroxidase was dropwise added to the sections, and they were incubated at 37°C for 30 min to enable the labeled peroxidase to bind to the fluorescein-labeled nucleotides. After the PBS washes, the sections were incubated with a diaminobenzidine (DAB) substrate for visualization prior to nuclear counterstaining with hematoxylin. Finally, the sections were sealed and observed/photographed under a microscope (Olympus). The nuclei of the apoptotic cells were stained brown. Five high-magnification view fields were selected for calculating the apoptotic index.

### *TEM examination*

The 2.5% glutaraldehyde-fixed umbilical arterial segments were washed with PBS solution and fixed in 1% osmic acid for 1 h. The tissue was then washed with phosphate-buffered solution and dehydrated using a gradient of acetone solutions, followed by Epon812 embedding and polymerization at 60°C for 24 h. After localization on semi-thin transverse sections was observed under an optical microscope, 90-nm-thick ultrathin sections were prepared and placed onto a copper grid with a supported membrane. After a 10-min staining with 5% aqueous sodium uranyl acetate and a 5-min staining with lead citrate, TEM (Leo906) observation was conducted to examine the vascular wall ultrastructure.

### *Statistical analysis*

The statistical analyses were performed using SPSS 21.0 (SPSS, Chicago, IL, USA). Measure-

## The chick embryo umbilical artery vasospasm model

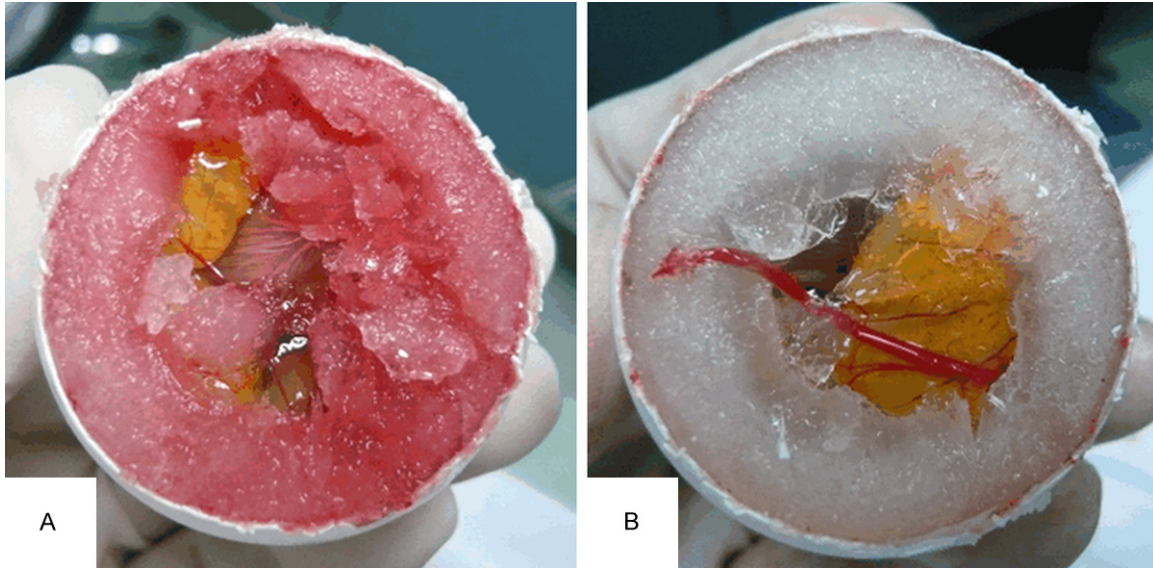


**Figure 3.** Gross anatomical images of the chicken embryonated eggs that were sacrificed on day 1 post-hemorrhage by freezing them at  $-80^{\circ}\text{C}$  for 30 min. A. Experimental group: the allantoic fluid appeared bloody red; B. Control group: the allantoic fluid appeared colorless.

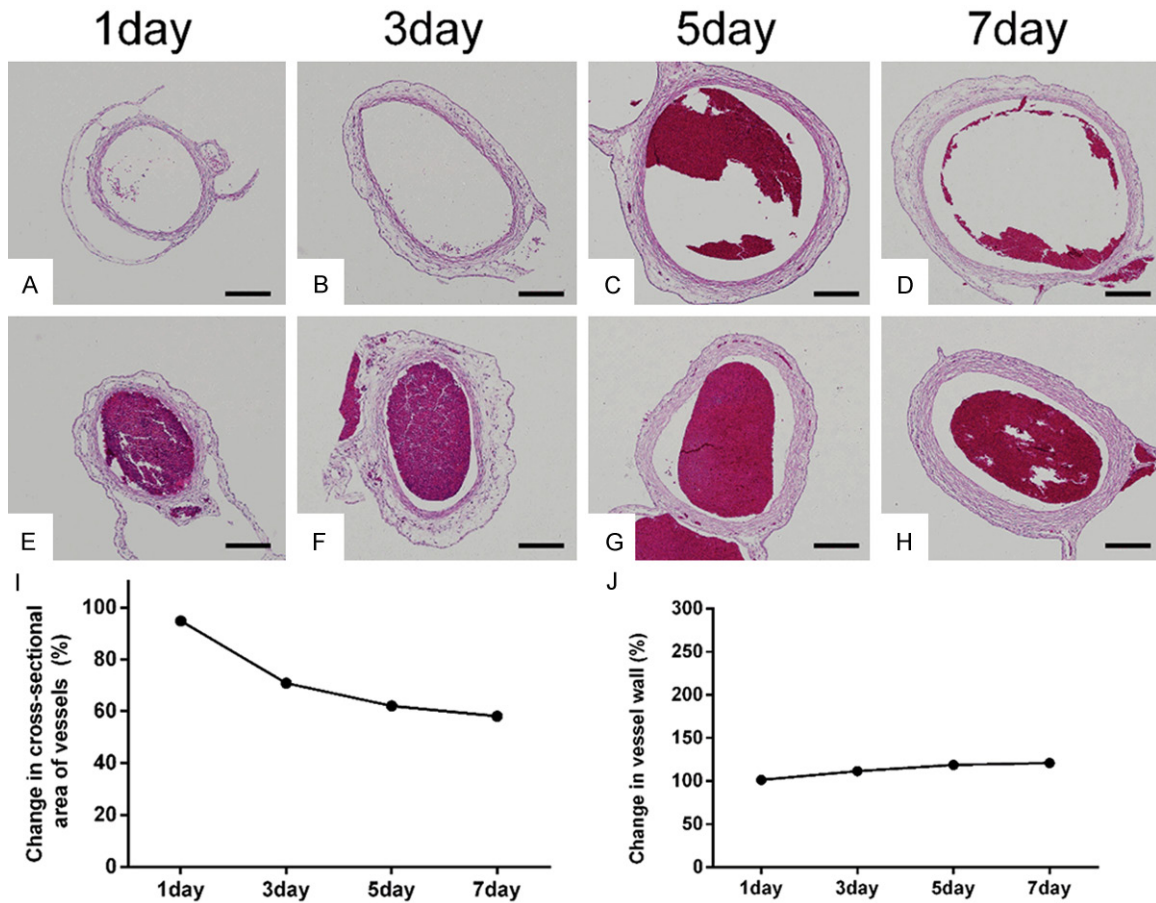


**Figure 4.** A-D. Show representative pathological images of the umbilical artery in the allantoic cavity of the control group on days 1, 3, 5, and 7 post-hemorrhage, respectively; E-H. Show the representative pathological images of the umbilical artery in the allantoic cavity of the control group on days 1, 3, 5, and 7 post-hemorrhage, respectively

## The chick embryo umbilical artery vasospasm model

(scale bar = 100  $\mu\text{m}$ ); I. Shows the trend of the mean umbilical arterial inner CSA ratio between the experimental group and the control group; J. Shows the trend of the mean umbilical arterial wall thickness ratio between the experimental group and the control group.

**Table 2.** Inner CSA ( $\mu\text{m}^2$ ) of the two groups

	Day 1	Day 3	Day 5	Day 7
Control group	42056.73 $\pm$ 1937.07	80244.47 $\pm$ 3092.58	143656.90 $\pm$ 2989.76	151560.10 $\pm$ 3062.12
Experimental group	39885.69 $\pm$ 1789.15	56889.52 $\pm$ 2094.63	89161.97 $\pm$ 2157.81	88019.20 $\pm$ 2014.49
P value	0.085	0.007	0.000	0.000

Abbreviations: CSA, cross-sectional area.

**Table 3.** Vascular wall thickness ( $\mu\text{m}$ ) of the two groups

	Day 1	Day 3	Day 5	Day 7
Control group	25.40 $\pm$ 1.35	31.45 $\pm$ 1.42	43.94 $\pm$ 1.79	44.40 $\pm$ 1.63
Experimental group	25.77 $\pm$ 1.47	35.04 $\pm$ 1.49	52.11 $\pm$ 1.84	53.71 $\pm$ 1.81
P value	0.677	0.002	0.000	0.000

*Changes in the inner CSA and wall thickness of the blood vessels*

The inner CSA was measured independently by two researchers using images of the pathological sections.

ment data was represented as  $\bar{x} \pm s$  while T test was used for the comparison between two groups on measuring data.  $P < 0.05$  referred to statistically significant differences.

### Results

#### *Needle puncture-associated chicken embryo death rate during modeling*

During the hatching of the chicken embryonated eggs, one egg each failed to hatch in the control and experimental groups and was replaced with an embryonated egg from the reserve supply. Daily observation of the eggs after puncture-induced hemorrhage by candling revealed no chicken embryo deaths in the control group and 13 deaths in the experimental group, including 11 deaths on day 1 after puncture-induced hemorrhage (2 in subgroup day 1, 3 in subgroup day 3, 4 in subgroup day 5, 2 in subgroup day 7), one death on day 2 (subgroup day 7), and one death on day 3 (subgroup day 7). The death rates of the two groups are shown in **Table 1**.

#### *Gross anatomical observation*

On day 1 post-hemorrhage, the chicken embryonated eggs in the experimental and control groups were sacrificed by freezing them at  $-80^\circ\text{C}$  for 30 min and dissected for observation. The allantoic fluid in the allantoic cavity appeared bloody red in the experimental group and colorless in the control group (**Figure 3**).

The inner CSA measurements of the three segments (the proximal, distal, and middle segments) were averaged, and the results from the two researchers were averaged to obtain the final inner CSA values (a representative section is shown in **Figure 4**). The wall thicknesses were calculated based on the measured inner and outer CSAs using a geometric formula. The CSA and wall thickness values of the control and experimental groups on days 1, 3, 5, and 7 post-hemorrhage are displayed in **Tables 2 and 3**. Compared with the control group, the average inner CSA of the experimental group showed a statistically insignificant difference on day 1 post-hemorrhage but was significantly smaller on days 3, 5, and 7 post-hemorrhage ( $P < 0.05$ ). There was no statistically significant difference in wall thickness between the two groups on day 1 post-hemorrhage, but the wall thickness was remarkably greater in the experimental versus control group on days 3, 5, and 7 post-hemorrhage ( $P < 0.05$ ). The ratio of the mean CSA in the experimental group to that in the control group was used to represent the degree of vasospasm. The inner CSA of the umbilical artery in the allantoic cavity notably decreased on day 3 post-hemorrhage and reached a lowest point on day 7 post-hemorrhage (**Figure 4I**). The ratio of the mean wall thickness of the experimental group to the control group showed an increasing trend, suggesting a gradual increase in wall thickness after puncture-caused hemorrhage (**Figure 4J**).

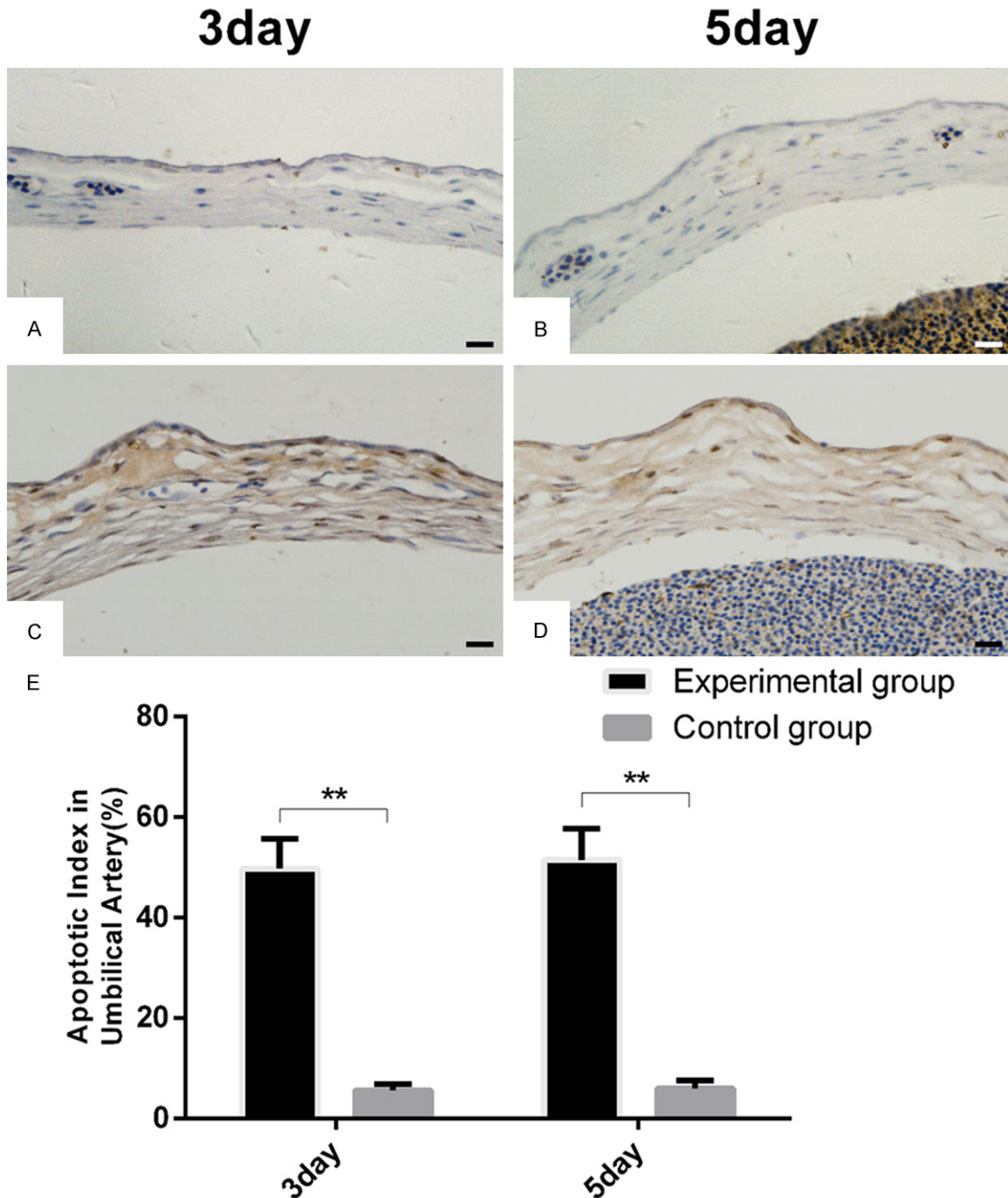


**Figure 5.** A and B. Show the TUNEL staining results of the umbilical arterial sections in the control group on post-hemorrhage days 3 and 5, respectively, in which the number of TUNEL-positive cells is extremely small; C and D. Show the TUNEL staining results of the umbilical arterial sections in the experimental group on post-hemorrhage days 3 and 5, respectively, in which the number of TUNEL-positive cells is substantial (scale bar = 20  $\mu$ m); E. Indicates that, as detected by TUNEL staining of the umbilical arterial sections, the apoptotic indexes of the experimental group on days 3 and 5 post-hemorrhage were significantly higher than those of the control group,  $**P < 0.01$ .

#### TUNEL staining

TUNEL staining of the umbilical arterial sections revealed that the number of TUNEL-

positive apoptotic cells on days 3 and 5 post-hemorrhage was significantly higher in the experimental versus the control group, with the control group having extremely low counts. The

## The chick embryo umbilical artery vasospasm model

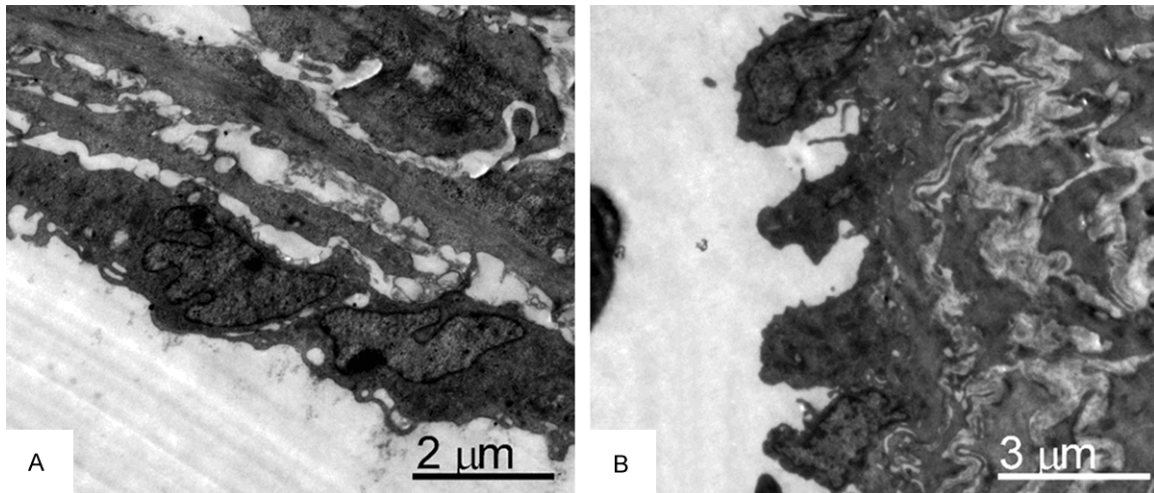


**Figure 6.** TEM observations of the umbilical artery on day 5 post-hemorrhage. A. Control group: the endothelial cells are arranged in a single layer with tight intercellular connections, the nuclei are oval, and the subendothelial layers are evenly arranged and clearly structured; B. Experimental group: the shrunken endothelial cells remain distributed in a single-layer pattern but are loosely arranged, and their normal intercellular connections are absent. The fragmented nuclear chromatin aggregates toward the nuclear membrane, and the subendothelial elastic layer displays wrinkles in a wavy pattern.

presence of TUNEL-positive material was not limited to vascular endothelial cells, and TUNEL-positive apoptotic cells were distributed throughout all the layers of the vascular wall. In addition, the apoptotic index of the experimental group was significantly higher than that of the control group ( $P < 0.01$ ) (Figure 5).

### *TEM observation of changes in the vascular ultrastructure*

On day 5 post-hemorrhage, TEM observation of the control group umbilical arteries showed endothelial cells with oval nuclei arranged in a single layer with tight intercellular connections, and the subendothelial layer was regularly arranged with a clear structure. In the experimental group, the endothelial cells remained distributed in a single-layer pattern; however, the endothelial cells were shrunken and loosely arranged, and their normal intercellular connections were absent. In addition, their fragmented nuclear chromatin aggregated toward the nuclear membrane and their subendothelial elastic layer exhibited wrinkles in a wavy pattern (Figure 6).

### **Discussion**

The allantoic sac of a chicken embryo originates from a bulge on the ventral side of the embryo on day 3.5 of incubation, which forms a

fluid-filled sac structure after rapid enlargement that wraps the entire embryo on day 10 of incubation. The proximal side of the sac is connected to the ventral side of the embryo with the wrapped umbilical artery and vein inside it. After coursing a certain distance in the allantoic cavity, the umbilical artery splits into two branches and enters the CAM, where its hierarchical branches form a dense vascular network that ultimately converges with the CAM vein. Blood returns to the main embryonic body through the umbilical vein [13, 14]. Because the fluid environment surrounding the allantoic artery is similar to the subarachnoid cerebrospinal fluid (CSF) environment surrounding the basicranial cerebral vessels, we attempted to simulate the post-SAH pathological changes associated with CVS in mammalian models by inducing umbilical arterial vasospasm through a CAM vein puncture method that causes internal bleeding in the allantoic cavity. Because chicken embryonated eggs require 10 days of hatching for allantoic closure, we chose 11-day-old chicken embryonated eggs as study subjects, wherein a complete allantoic circulation system had been established, as indicated by anastomosed and thicker CAM vessels, which allowed for relatively straightforward experimentation. Gross anatomical observation of the allantoic hemorrhage model on day 1 post-hemorrhage verified a remarkable level of inter-



## The chick embryo umbilical artery vasospasm model

nal bleeding in the allantoic cavity of the chicken embryo. Therefore, this method is feasible despite a puncture-associated chicken embryo death rate of approximately 36.11% (13/36) in the experimental group.

The most direct characteristics of vasospasm are decreased vascular CSA and a thicker vascular wall. Our experimental results showed that the inner CSA of the umbilical artery decreased by 5.16%, 29.10%, 37.93%, and 41.92% and the wall thickness increased by 1.46%, 11.42%, 18.59%, and 20.98% on days 1, 3, 5, and 7, respectively, after a hemorrhage in the allantoic cavity of the chicken embryo. These results indicate that vasospasm gradually deteriorated and reached a peak at day 7, which was clearly associated with the hemorrhage in the allantoic cavity of the chicken embryo. This finding is not completely consistent with those of other mammalian post-SAH CVS models. For example, in mouse endovascular puncture models, induced vasospasm achieved an approximately 20-62% luminal narrowing of the cerebral vessels, with a peak on the third day and general alleviation after one week [15-17]. In rat double-hemorrhage models, a hemorrhage (0.3 ml) induced vasospasm with a maximum of 47% luminal narrowing, which peaked at day 7 [8, 18]. In rabbit CVS models, an induced vasospasm achieved approximately 19-55% luminal narrowing and peaked at day 3 in single-hemorrhage models and at days 4-6 in double-hemorrhage models [19, 20]. Compared with a sham operation group, induced vasospasm in canine double-hemorrhage models resulted in 45-66% luminal narrowing of the vessels, which peaked on day 7 in the majority of studies [21, 22].

Pathoanatomical examination of aSAH patients who died from severe vasospasm found notable apoptotic changes in their endothelial cells and a wavy shrinkage of the elastic layer of the vascular wall [23]. Similar findings have also been observed in mammalian arterial models [24, 25]. The apoptosis of endothelial cells results in a reduction of vasodilator substances (i.e., nitric oxide (NO) and prostacyclin), which leads to blood-brain barrier damage and the exposure of the smooth-muscle layer to vasoconstrictor substances in the blood. This mechanism plays an important role in CVS and brain damage. In the present study, TUNEL staining

was conducted to investigate the apoptotic changes of the cells in the umbilical arterial wall, focusing on days 3 and 5 post-hemorrhage because the umbilical arterial vasospasm induced by puncture-caused hemorrhage in the allantoic cavity occurred on day 3 and reached its peak on days 5-7 post-hemorrhage. TUNEL-positive cells were widely apparent in both the endothelial and smooth-muscle layers of the umbilical arteries in the experimental group but very sparsely evident in the control group. The apoptotic index, detected by TUNEL staining of the umbilical arterial sections, was significantly higher in the experimental group compared with the control group. TEM observation of the umbilical arteries in the experimental group on day 5 post-hemorrhage demonstrated that the shrunken endothelial cells were still arranged in a single layer but had lost their normal intercellular connections and were loosely arranged, the fragmented nuclear chromatin aggregated toward the nuclear membrane, and the subendothelial elastic layer demonstrated a pattern of wavy wrinkles. These pathological changes are similar to those found in human post-aSAH and mammalian CVS models.

As the non-mammalian vertebrate phylogenetically closest to human beings, the chicken has been broadly used in biomedical research. With the deciphering of the chicken genome and the development of transgenic technology for chickens, the application of chicken models is likely to attract an increasing amount of attention. Compared with previous mammalian vasospasm models, our chicken embryo umbilical arterial vasospasm model demonstrates a variety of advantages, such as straightforward operation and cultivation, low cost, a short experimental cycle, and relatively few ethical constraints. However, our study also has intrinsic shortcomings. For example, chickens are phylogenetically farther from human beings than mammals, leading to the question of whether the results derived from chicken embryo models can be applied to humans and whether they might require further verification using mammalian or primate models. The hatching duration of a chicken embryo is 21 days, and allantoic closure is completed after the establishment of an allantoic circulation system evidenced by anastomosed and remarkably thicker CAM vessels after 10 days of hatching. The allantoic sac gradually shrinks and

## The chick embryo umbilical artery vasospasm model

loses its function after 19 days of egg hatching [13, 14]. As a result, the length of the research window is only approximately one week. In addition, the umbilical artery in the allantoic cavity is not an intracranial vessel; thus, it is not suitable for research on brain damage-accompanied vasospasm. However, this simple and low-cost vasospasm model is a useful tool for the exploration of pathogenesis and early drug screening for vasospasm and can minimize the use of mammalian models.

### Acknowledgements

This work was supported by the National Natural Science Foundation of China (81200-888).

### Disclosure of conflict of interest

None.

**Address correspondence to:** Jinlu Yu and Qi Luo, Department of Neurosurgery, First Hospital of Jilin University, 71 Xinmin Avenue, Changchun 130021, China. E-mail: jinluyu@hotmail.com

### References

- [1] Becker KJ. Epidemiology and clinical presentation of aneurysmal subarachnoid hemorrhage. *Neurosurg Clin N Am* 1998; 9: 435-444.
- [2] Wardlaw JM and White PM. The detection and management of unruptured intracranial aneurysms. *Brain* 2000; 123: 205-221.
- [3] Dorsch NW. Cerebral arterial spasm—a clinical review. *Br J Neurosurg* 1995; 9: 403-412.
- [4] Przybycien-Szymanska MM and Ashley WW Jr. Biomarker Discovery in Cerebral Vasospasm after Aneurysmal Subarachnoid Hemorrhage. *J Stroke Cerebrovasc Dis* 2015; 24: 1453-64.
- [5] Wilkins RH. Cerebral vasospasm. *Crit Rev Neurobiol* 1990; 6: 51-77.
- [6] Titova E, Ostrowski RP, Zhang JH and Tang J. Experimental models of subarachnoid hemorrhage for studies of cerebral vasospasm. *Neurol Res* 2009; 31: 568-581.
- [7] Marbacher S, Fandino J and Kitchen ND. Standard intracranial in vivo animal models of delayed cerebral vasospasm. *Br J Neurosurg* 2010; 24: 415-434.
- [8] Marbacher S, Fandino J and Kitchen N. Characteristics of in vivo animal models of delayed cerebral vasospasm. *Acta Neurochir Suppl* 2011; 110: 173-175.
- [9] Coleman CM. Chicken embryo as a model for regenerative medicine. *Birth Defects Res C Embryo Today* 2008; 84: 245-256.
- [10] Deryugina EI and Quigley JP. Chick embryo chorioallantoic membrane model systems to study and visualize human tumor cell metastasis. *Histochem Cell Biol* 2008; 130: 1119-1130.
- [11] Chiba A, Yui C and Hirano S. Liver reconstruction on the chorioallantoic membrane of the chick embryo. *Arch Histol Cytol* 2010; 73: 45-53.
- [12] Liu M, Scanlon CS, Banerjee R, Russo N, Inglehart RC, Willis AL, Weiss SJ and D'Silva NJ. The Histone Methyltransferase EZH2 Mediates Tumor Progression on the Chick Chorioallantoic Membrane Assay, a Novel Model of Head and Neck Squamous Cell Carcinoma. *Transl Oncol* 2013; 6: 273-281.
- [13] Yuan YJ, Xu K, Wu W, Luo Q and Yu JL. Application of the chick embryo chorioallantoic membrane in neurosurgery disease. *Int J Med Sci* 2014; 11: 1275-1281.
- [14] Tufan AC and Satiroglu-Tufan NL. The chick embryo chorioallantoic membrane as a model system for the study of tumor angiogenesis, invasion and development of anti-angiogenic agents. *Current Cancer Drug Targets* 2005; 5: 249-266.
- [15] Kamii H, Kato I, Kinouchi H, Chan PH, Epstein CJ, Akabane A, Okamoto H and Yoshimoto T. Amelioration of vasospasm after subarachnoid hemorrhage in transgenic mice overexpressing CuZn-superoxide dismutase. *Stroke* 1999; 30: 867-871; discussion 872.
- [16] McGirt MJ, Parra A, Sheng H, Higuchi Y, Oury TD, Laskowitz DT, Pearlstein RD and Warner DS. Attenuation of cerebral vasospasm after subarachnoid hemorrhage in mice overexpressing extracellular superoxide dismutase. *Stroke* 2002; 33: 2317-2323.
- [17] Lin CL, Calisaneller T, Ukita N, Dumont AS, Kassell NF and Lee KS. A murine model of subarachnoid hemorrhage-induced cerebral vasospasm. *J Neurosci Methods* 2003; 123: 89-97.
- [18] Vatter H, Weidauer S, Konczalla J, Dettmann E, Zimmermann M, Raabe A, Preibisch C, Zanella FE and Seifert V. Time course in the development of cerebral vasospasm after experimental subarachnoid hemorrhage: clinical and neuroradiological assessment of the rat double hemorrhage model. *Neurosurgery* 2006; 58: 1190-1197; discussion 1190-1197.
- [19] Chan RC, Durity FA, Thompson GB, Nugent RA and Kendall M. The role of the prostacyclin-thromboxane system in cerebral vasospasm following induced subarachnoid hemorrhage in the rabbit. *J Neurosurg* 1984; 61: 1120-1128.
- [20] Ahmad I, Imaizumi S, Shimizu H, Kaminuma T, Ochiai N, Tajima M and Yoshimoto T. Development of calcitonin gene-related peptide slow-

## The chick embryo umbilical artery vasospasm model

- release tablet implanted in CSF space for prevention of cerebral vasospasm after experimental subarachnoid haemorrhage. *Acta Neurochir (Wien)* 1996; 138: 1230-1240.
- [21] Chyatte D. Prevention of chronic cerebral vasospasm in dogs with ibuprofen and high-dose methylprednisolone. *Stroke* 1989; 20: 1021-1026.
- [22] Zhou C, Yamaguchi M, Kusaka G, Schonholz C, Nanda A and Zhang JH. Caspase inhibitors prevent endothelial apoptosis and cerebral vasospasm in dog model of experimental subarachnoid hemorrhage. *J Cereb Blood Flow Metab* 2004; 24: 419-431.
- [23] Zubkov AY, Ogihara K, Bernanke DH, Parent AD and Zhang J. Apoptosis of endothelial cells in vessels affected by cerebral vasospasm. *Surg Neurol* 2000; 53: 260-266.
- [24] Zubkov AY, Tibbs RE, Aoki K and Zhang JH. Morphological changes of cerebral penetrating arteries in a canine double hemorrhage model. *Surg Neurol* 2000; 54: 212-219; discussion 219-220.
- [25] Zubkov AY, Tibbs RE, Clower B, Ogihara K, Aoki K and Zhang JH. Morphological changes of cerebral arteries in a canine double hemorrhage model. *Neurosci Lett* 2002; 326: 137-141.